

Substrate Removed GaAs–AlGaAs Electrooptic Modulators

S. R. Sakamoto, A. Jackson, and N. Dagli

Abstract—A novel GaAs–AlGaAs electrooptic modulator utilizing push–pull metal electrodes was fabricated using substrate removal techniques and polymer integration. The scheme enables a significant drive voltage reduction over previous designs and should enable ultrahigh-speed adjustable chirp operation.

Index Terms—Electrooptic modulators, GaAs modulators, optical modulators.

I. INTRODUCTION

ULTRAWIDE-BANDWIDTH low-voltage external modulators with adjustable chirp are essential for digital and analog fiber optic transmission. Our previous work on GaAs–AlGaAs designs utilizing novel slow wave T-rail electrodes [1] and undoped epilayers were able to obtain chirp-free modulation in excess of 40 GHz [2]. But the drive voltage (V_π) of these modulators was 16.8 V at 1.55 μm , which was high for high speed operation. The high V_π was mainly due to the poor overlap of the vertical electric field component of the modulating field with the optical mode. Recently, substrate removal techniques enabled processing both sides of epitaxial layers and successful integration of semiconductors and polymers for optoelectronic applications [3]. Here, we present an electrooptic modulator that takes advantage of these new technologies to reduce V_π by a factor of 2.

II. DEVICE DESCRIPTION

Figs. 1 and 2 show the top and cross-sectional schematics of the modulator, respectively. The optical structure is a Mach–Zehnder interferometer. The input and output of the interferometer use 1×2 multimode interference (MMI) couplers [4]. The optical waveguides are rib waveguides. The epitaxial structure is an undoped GaAs–Al_{0.3}Ga_{0.7}As heterostructure grown by MBE on a semi-insulating (SI) GaAs substrate. There are electrodes at the top and bottom of both arms of the interferometer. These electrodes form Schottky diodes. The electrodes on each arm can be biased independently. The voltage across an arm biases two back to back Schottky diodes and makes it possible to apply a vertical electric field component overlapping very well with the optical mode in the single mode rib waveguide. Such epilayers are self-depleting due to Fermi level pinning at the surface and the SI

Manuscript received May 3, 1999; revised July 2, 1999. This work was supported by Air Force Office of Scientific Research under Grant F19628-97-C-0069.

The authors are with the Electrical and Computer Engineering Department, University of California, Santa Barbara, CA 93106 USA.

Publisher Item Identifier S 1041-1135(99)07774-5.

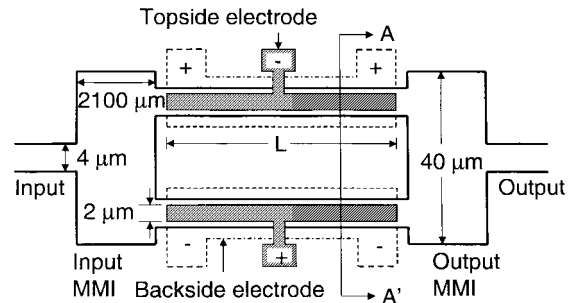


Fig. 1. Schematic view of the modulator as seen from transfer substrate up along BB' in.

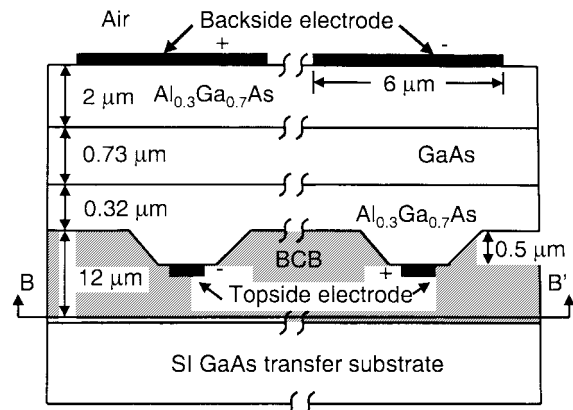


Fig. 2. As described in the Section III topside refers to the top of the as-grown epilayer and backside refers to the interface between the lower cladding and the growth substrate. Backside is exposed to air after the growth substrate is removed. Cross section $A-A'$ of the substrate removed modulator.

substrate interface, and therefore have very low conductivity. For time varying voltages they start to behave as slightly lossy dielectrics and the situation becomes very similar to the case of electrodes on a dielectric material. Therefore, push–pull vertical electric fields overlapping very well with the optical mode can be applied. The strength of the field is limited only by the thickness of the epilayer. The electrodes can be shaped as T-rails and combined with coplanar electrodes for high speed traveling wave modulators [1].

V_π of such a device can be expressed as

$$V_\pi = \frac{\lambda}{2L} \frac{t}{n^3 r_{41}} \frac{1}{\Gamma} \quad (1)$$

where Γ is the overlap between the vertical component of the applied electric field and the optical mode. $r_{41} = 1.4 \times 10^{-12}$ m/V and $n = 3.4$ are the electrooptic coefficient and optical

index of the AlGaAs material, respectively, L is the length of the electrode, λ is the wavelength of operation and $t = 3.55 \mu\text{m}$ is the overall thickness of the epilayer.

III. DEVICE FABRICATION

The fabrication begins with the MBE growth of an appropriately designed, undoped epilayer for single-mode waveguide operation at $1.55 \mu\text{m}$. The epilayer schematic is shown in Fig. 2. Between the epilayer and the growth substrate, a $0.1\text{-}\mu\text{m}$ AlAs etch stop layer was also grown. Using standard photolithography, the Mach–Zehnder structure is patterned and wet etched using a citric acid solution. The waveguides are $4 \mu\text{m}$ wide and etched $0.5 \mu\text{m}$ deep. $2\text{-}\mu\text{m}$ -wide metal electrodes are then patterned on top of both $4\text{-}\mu\text{m}$ waveguides in the interaction region using Ti–Pt–Au–Schottky metal liftoff. Each electrode has its own contact pad for independent probing. At this point, the processing of the topside of the epi is complete.

The next step was the transfer of the processed epilayer onto a transfer substrate. We chose a SI GaAs as the transfer substrate because it was readily available and allowed easy facet formation with cleaving. Any other optically flat substrate such as quartz can be used if facets are formed using reactive ion etching. To glue the epilayer to the transfer substrate, we used the organic polymer benzocyclobutene (BCB).¹ BCB was spun both onto the transfer substrate and on top of the processed epilayer. The sample was then placed epi-side down onto the transfer substrate kept on a hot plate at $160 \text{ }^\circ\text{C}$. At this temperature, the BCB became less viscous and allowed easy sliding of the semiconductors. This was essential for the manual alignment of the cleavage planes of the transfer and growth substrates and also for the removal of any voids or gas bubbles that may have been trapped. After this alignment the BCB was fully cured at $250 \text{ }^\circ\text{C}$ for 1 h in a nitrogen purged oven. A spray etch of an ammonium hydroxide/hydrogen peroxide mixture was used to remove the growth substrate. The etch stopped on an AlAs etch stop layer. Once the AlAs layer was removed, the processing of the backside began.

In the processing of the backside, first the topside alignment marks were exposed through the epi. This was done using a back aligner with infrared (IR) illumination and an IR camera. The epilayer around the topside alignment marks were etched using a citric acid solution. Next, Schottky Ti–Pt–Au backside electrodes were patterned using lift off. These electrodes were aligned directly underneath the topside electrodes. Each of these electrodes had an independent contact pad for probing. The last mask used was to define and etch the epilayer on the buried topside electrode contact pads for probing. Finally, the sample was cleaved and mounted.

IV. EXPERIMENTAL RESULTS

Electrical measurements between two contacts across an arm showed back to back diode characteristics as expected. The reverse breakdown voltage of the diodes was larger than 40 V. The current through an $L = 0.5\text{-cm}$ -long electrode

¹Form No: 296-01 211-493NP&M, Dow Plastics, The Dow Chemical Company, 2040 Dow Center, Midland, MI 48674 USA.

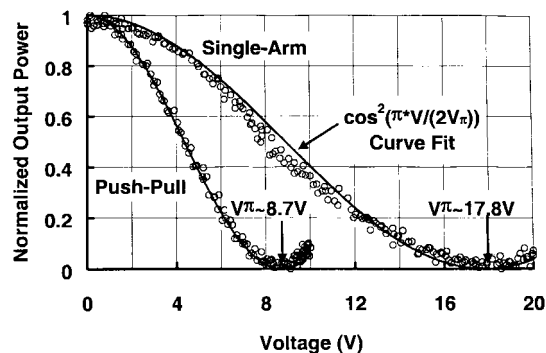


Fig. 3. 10-kHz transfer function of $L = 1\text{-cm}$ modulator.

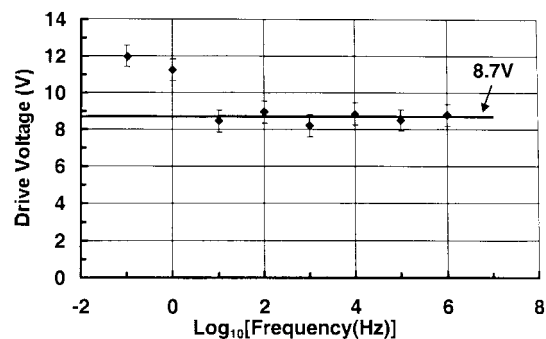


Fig. 4. Drive voltage of $L = 1\text{-cm}$ modulator as a function of frequency.

was less than $30 \mu\text{A}$ at 30 V. For optical characterization, the output of a fiber pigtailed $1.55\text{-}\mu\text{m}$ distributed-feedback laser was end fire coupled through the cleaved facet. Input polarization was controlled using a three-paddle polarization rotator and was kept at TE polarization during the measurements. At the output facet, the near-field pattern was observed by focusing the image through a microscope objective onto an IR Vidicon camera. Output power was measured by aligning a cleaved fiber to the output port of the modulator and feeding the signal to a Tektronix 11403A Digitizing Oscilloscope via a Tek P6702 Optical/Electric Converter. Since each electrode had its own contact pad, four probes were used to provide a push–pull biasing scheme. A function generator was used to provide 20-V sinusoidal modulation up to 1 MHz.

The loss coefficient of passive straight waveguides on the same chip was measured to be about 0.5 dB/cm. The loss coefficient of the straight phase modulators, which are straight waveguides with electrodes on both sides, increased to about 5 dB/cm. This increase is mainly due to the close proximity of the topside electrode and can be eliminated by increasing the upper cladding thickness [5]. The overall on chip loss of the modulator was about 7 dB for a chip length of 2 cm. The cleaved fiber to cleaved fiber insertion loss was about 23 dB due to an additional 16-dB loss originating from mode mismatch and facet reflections. This additional loss can be decreased significantly using tapered transitions to polymer waveguides.

The 10-kHz transfer functions of a device with a 1-cm interaction region when driven push–pull and single-arm only are shown in Fig. 3. The transfer functions follow the expected \cos^2 shape. Push–pull operation reduces V_π by a factor of 2

from 17.8 to 8.7 V. In addition, the $L = 1$ cm V_{π} of 8.7 V is about a factor of 2 smaller than the previous ultrahigh-speed traveling-wave modulator [2]. V_{π} of a push-pull driven $L = 0.5$ -cm modulator is 17.8 V as expected. Fig. 4 shows the V_{π} of $L = 1$ -cm device as a function of frequency. As expected at very low frequencies applied field strength and overlap with the optical mode is determined by the extent of the depletion layers. In order for the depletion layer to respond to the applied field, charge has to be pushed in and out of the device. This charge can either be supplied by the external circuit or from somewhere else in the epilayer. In this case there is no charge injection or removal from the external circuit because of back-to-back Schottky barriers. There is also very little charge in the epilayer due to self-depletion. So when the polarity of the voltage changes on an electrode and the area under that electrodes should no longer be depleted, required charge can only come from thermal generation. This is a very slow process and when the voltage changes rapidly there is no time for that to happen and the epilayer remains depleted all the time. As a result over 10 Hz, the epilayer starts to behave as a slightly lossy dielectric and (1) becomes applicable. These results imply a 58% overlap between the electrode field and the optical mode using (1). Numerical simulations using the geometry shown on half of Fig. 2 and treating it as pure dielectric material predict 60% overlap, which is in good agreement with the experimental result. These simulations also indicate it is possible to increase this overlap to close to 90% by widening the electrode and optimizing the optical waveguide. This should bring V_{π} to about 5.5 V-cm, which is comparable to existing LiNbO_3 modulators. As described

earlier these devices can be combined with coplanar slow wave electrodes to realize ultrawide-bandwidth traveling-wave modulators.

V. CONCLUSION

Substrate removal techniques enabled us to process both sides of an epilayer and integrate it with organic polymers. Using this approach we fabricated novel substrate removed Mach-Zehnder GaAs-AlGaAs electrooptic modulators using undoped epilayers. The modulators have 8.7 V-cm drive voltage, which can be further improved to 5.5 V-cm. The arms of these modulators can be biased independently making it possible to adjust their chirp over a wide range. These devices can be made ultrahigh speed using T-rail loaded coplanar slow-wave electrodes.

REFERENCES

- [1] S. Sakamoto, R. Spickermann, and N. Dagli, "Novel narrow gap coplanar slow wave electrode for traveling wave electrooptic modulators," *Electron. Lett.*, vol. 31, no. 14, pp. 1183-1185, July 6, 1995.
- [2] R. Spickermann, S. R. Sakamoto, M. G. Peters, and N. Dagli, "GaAs/AlGaAs traveling wave electro-optic modulator with an electrical bandwidth >40 GHz," *Electron. Lett.*, vol. 32, no. 12, pp. 1095-1096, June 1996.
- [3] S. R. Sakamoto, C. Ozturk, Y. T. Byun, J. Ko, and N. Dagli, "Low-loss substrate removed (SURE) optical waveguides in GaAs-AlGaAs epitaxial layers embedded in organic polymers," *IEEE Photon. Technol. Lett.*, vol. 10, pp. 985-987, July 1998.
- [4] L. B. Soldano and E. C. M. Pennings, "Optical multi-mode interference devices based on self-imaging: Principles and applications," *J. Lightwave Technol.*, vol. 13, pp. 615-627, Apr. 1995.
- [5] A. Bek, A. Aydinli, J. G. Champlain, R. Naone, and N. Dagli, "A study of wet oxidized $\text{Al}_x\text{Ga}_{1-x}\text{As}$ for integrated optics," *IEEE Photon. Technol. Lett.*, vol. 11, pp. 436-438, Apr. 1999.